CORRECTION

Doublecortin marks a new population of transiently amplifying muscle progenitor cells and is required for myofiber maturation during skeletal muscle regeneration

Ryo Ogawa, Yuran Ma, Masahiko Yamaguchi, Takahito Ito, Yoko Watanabe, Takuji Ohtani, Satoshi Murakami, Shizuka Uchida, Piera De Gaspari, Akiyoshi Uezumi, Miki Nakamura, Yuko Miyagoe-Suzuki, Kazutake Tsujikawa, Naohiro Hashimoto, Thomas Braun, Teruyuki Tanaka, Shin'ichi Takeda, Hiroshi Yamamoto and So-ichiro Fukada

There was an error published in *Development* **142**, 51-61.

In the Discussion (p. 57), it was stated that: Pallafacchina et al. reported that Dcx is expressed in neonatal satellite cells but not in adult satellite cells (Pallafacchina et al., 2010). This should have stated: Pallafacchina et al. reported that Dcx is expressed in satellite cells from one-week-old mice and adult mice depleted for dystrophin, where satellite cells are reactivated, but not (or at only very low levels) in resting satellite cells in the wild-type adult or in activated myoblasts in culture (Pallafacchina et al., 2010).

The authors apologise to readers for this mistake.

Doublecortin marks a new population of transiently amplifying muscle progenitor cells and is required for myofiber maturation during skeletal muscle regeneration

Ryo Ogawa[1],*, Yuran Ma[1],*, Masahiko Yamaguchi[1], Takahito Ito[1], Yoko Watanabe[1], Takuji Ohtani[1], Satoshi Murakami[1], Shizuka Uchida[2], Piera De Gaspari[3], Akiyoshi Uezumi[4], Miki Nakamura[1], Yuko Miyagoe-Suzuki[5], Kazutake Tsujikawa[1], Naohiro Hashimoto[6], Thomas Braun[3], Teruyuki Tanaka[7], Shin'ichi Takeda[5], Hiroshi Yamamoto[1] and So-ichiro Fukada[1],‡

ABSTRACT

Muscle satellite cells are indispensable for muscle regeneration, but the functional diversity of their daughter cells is unknown. Here, we show that many Pax7^{+}MyoD^{−} cells locate both beneath and outside the basal lamina during myofiber maturation. A large majority of these Pax7^{+}MyoD^{−} cells are not self-renewed satellite cells, but have different potentials for both proliferation and differentiation from Pax7^{+}MyoD[+] myoblasts (classical daughter cells), and are specifically marked by expression of the doublecortin (Dcx) gene. Transplantation and lineage-tracing experiments demonstrated that Dcx-expressing cells originate from quiescent satellite cells and that the microenvironment induces Dcx in myoblasts. Expression of Dcx seems to be necessary for myofiber maturation because Dcx-deficient mice exhibited impaired myofiber maturation resulting from a decrease in the number of myonuclei. Furthermore, in vitro and in vivo studies suggest that one function of Dcx in myogenic cells is acceleration of cell motility. These results indicate that Dcx is a new marker for the Pax7^{+}MyoD[−] subpopulation, which contributes to myofiber maturation during muscle regeneration.

KEY WORDS: Satellite cells, Myofiber maturation, Regeneration, Doublecortin

INTRODUCTION

The discovery of skeletal muscle-specific basic helix-loop-helix transcription factors, i.e. MyoD (Myod1), Myf5, myogenin and Mrf4, allows us to distinguish the cells in each differential stage during myogenic differentiation (Sabourin and Rudnicki,

[1]Laboratory of Molecular and Cellular Physiology, Graduate School of Pharmaceutical Sciences, Osaka University, 1-6 Yamada-oka, Suita, Osaka 565-0871, Japan. [2]Institute of Cardiovascular Regeneration, Centre for Molecular Medicine, Goethe University Frankfurt, Theodor-Stern-Kai 7, Frankfurt am Main 60590, Germany. [3]Max Planck Institute for Heart and Lung Research, Ludwigstrasse 43, Bad Nauheim 61231, Germany. [4]Division for Therapies Against Intractable Diseases, Institute for Comprehensive Medical Science, Fujita Health University, 1-98 Dengakugakubo, Kutsukake, Toyoake, Aichi 470-1192, Japan. [5]Department of Molecular Therapy, National Institute of Neuroscience, National Center of Neurology and Psychiatry, 4-1-1 Ogawa-higashi, Kodaira, Tokyo 187-8502, Japan. [6]Department of Regenerative Medicine, National Institute for Longevity Sciences, National Center for Geriatrics and Gerontology, 35 Gengo, Morioka, Oobu, Aichi 474-8522, Japan. [7]Department of Developmental Medical Sciences, Graduate School of Medicine, University of Tokyo, 7-3-1 Hongo, Bunkyo-ku, Tokyo 113-0033, Japan.
*These authors contributed equally to this work

‡Author for correspondence (fukada@phs.osaka-u.ac.jp)

2000). Two paired box genes, Pax3 and Pax7, are also expressed in a differentiation-specific manner and are well known as essential transcription factors for skeletal muscle development (Buckingham, 2007). Although the expression of Pax3 marks some satellite cells in adult skeletal muscle (Relaix et al., 2006), all mitotically quiescent satellite cells (muscle stem cells) are marked by Pax7, but not by MyoD, myogenin or Mrf4. However, Myf5 is differentially expressed in satellite cells, and Myf5-negative satellite cells exhibit more stem cell characteristics than Myf5-positive satellite cells (Kuang et al., 2007).

When skeletal muscle is damaged, satellite cells start to express MyoD and expand to proliferate, at which time they are called myoblasts. MyoD-expressing cells subsequently express myogenin and lose Pax7 expression. Finally, they fuse with each other or a multinuclear myotube and eventually regenerate mature myofibers. Although the molecular mechanisms and timing of the generation of self-renewed satellite cells are controversial, a satellite cell population is maintained during the regenerative process to sustain the number of cells, and the Pax7^{+}MyoD[−] population is considered to comprise the self-renewed satellite cells. One self-renewal model was proposed by Zammit et al. Using an in vitro single-myofiber culture model, they demonstrated that almost all satellite cells become Pax7^{+}MyoD^{+} cells but that some of them revert to a Pax7^{+}MyoD[−] status to be able to function at the next occasion of muscle damage (Zammit et al., 2004). Asymmetric division has also been proposed as a model of self-renewal of satellite cells (Kuang et al., 2007). Whichever occurs, only Pax7^{+}MyoD^{+} cells are considered daughter cells derived from satellite cells before they start to express myogenin. Nevertheless, although a fundamental myogenic differentiation model has been established as described, in vivo skeletal muscle differentiation processes are not fully understood (Zammit, 2008).

In this study, we found that 5 days after damage by cardiotoxin injection, regenerating skeletal muscle has ∼10 times as many Pax7^{+}MyoD^{−} cells as before injury. Most Pax7^{+}MyoD^{−} cells express doublecortin (Dcx), but quiescent satellite cells and Pax7^{+}MyoD[+] proliferating myoblasts do not. Dcx^{+} cells originate from satellite cells, and Myf5^{−} satellite stem cells also express Dcx transcripts. Transplantation studies show that a specific microenvironment induces the expression of Dcx protein in classical proliferating myoblasts. Furthermore, studies of retrovirally induced Dcx-expressing myogenic cells or Dcx knockout mice suggest that Dcx contributes to the maturation of myofibers by promoting cell motility. Our findings suggest a new type of myogenic progenitor that will facilitate cellular regulation of satellite cells.

RESULTS

Pax7 and MyoD expression during muscle regeneration

When skeletal muscle is injured, satellite cells start to express MyoD and begin to proliferate, at which point they are known as myoblasts. After proliferation, they express myogenin and lose Pax7 expression, fuse with each other or nascent myotubes, and eventually regenerate mature myofibers (Fig. 1A). First, to reveal the expression patterns of both Pax7 and MyoD proteins *in vivo*, freshly isolated myogenic cells were stained using their specific antibodies (Fig. 1B). Regardless of regenerative stage, almost all the mononuclear myogenic cells can be enriched in the SM/C-2.6$^+$Sca-1$^-$CD31$^-$CD45$^-$ fraction (supplementary material Fig. S1A,B) as reported previously (Segawa et al., 2008), although there is a possibility that a very rare population is included in the all negative and Sca-1$^+$CD31$^-$CD45$^-$ fraction (supplementary material Fig. S1B). In the SM/C-2.6$^+$Sca-1$^-$CD31$^-$CD45$^-$ fraction, nearly all myogenic cells purified from muscle expressed both Pax7 and MyoD 2 days after receiving a cardiotoxin (CTX) injection (CTX-2d). However, the number of Pax7$^+$MyoD$^-$ myogenic cells peaked 5 days after CTX injection (CTX-5d). Pax7$^+$MyoD$^-$ is the typical expression pattern of self-renewed satellite cells, but the absolute number of Pax7$^+$MyoD$^-$ myogenic cells in CTX-5 muscles is ~10-fold higher than that in uninjured muscle (Fig. 1C). In addition, the low level of MyoD and high level of

Pax7 in CTX-5d myogenic cells when compared with CTX-2d myogenic cells were confirmed by transcriptional analyses (Fig. 1D). Myogenin was rarely detected in CTX-2d myogenic cells, but 25% of the CTX-3d myogenic cells expressed myogenin (supplementary material Fig. S1C).

We performed the same analyses using muscle sections. Although Pax7 expression was rarely detected in CTX-2d muscle, abundant Pax7$^+$MyoD$^-$ cells were detected 4-7 days after CTX injection (middle phase of regeneration) (Fig. 1E). The lack of Pax7 staining of the CTX-2d muscle seemed to be due to the low level of Pax7 expression compared with that in CTX-5d myogenic cells (Fig. 1D) or quiescent satellite cells (Cheung et al., 2012). Collectively, these results imply that most Pax7$^+$MyoD$^-$ cells in the middle phase of regeneration play one or more roles in the regeneration because their numbers were much larger compared with the number of satellite cells in uninjured muscles.

Functional differences between CTX-2d and CTX-5d myogenic cells

In order to assess the functional differences between CTX-2d and CTX-5d myogenic cells, first, an *in vivo* EdU (a thymidine analogue)-uptake assay was performed. As shown in Fig. 2A, ~60% of MyoD$^+$ cells were labeled by EdU in CTX-3d muscle during a 24 h pulse-chase experiment. The frequency of EdU$^+$
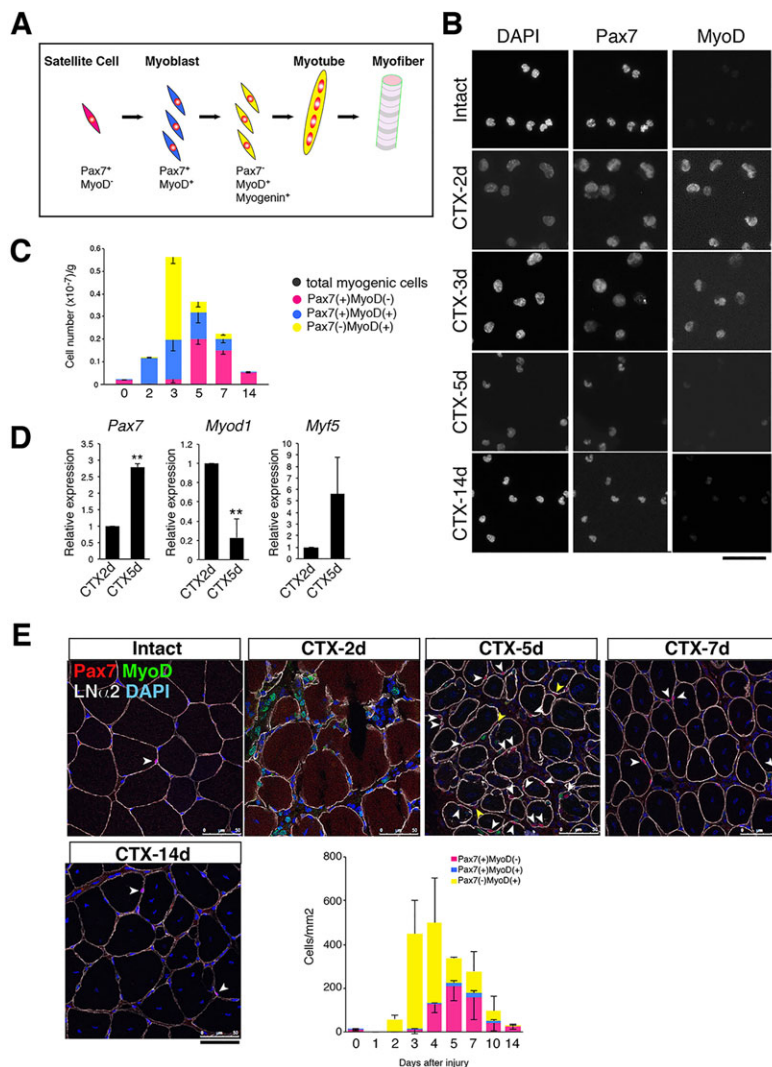

Fig. 1. Expression of Pax7 and MyoD during skeletal muscle regeneration. (A) The current myogenic differentiation model. (B) Immunostaining of Pax7 and MyoD in sorted myogenic cells derived from intact or CTX-damaged muscle. Nuclei were counterstained with DAPI. Scale bar: 50 μm. (C) The y-axis shows the number of Pax7$^+$MyoD$^-$ (pink), Pax7$^+$MyoD$^+$ (blue) or Pax7$^-$MyoD$^+$ (yellow) cells per gram of muscle weight±s.d. in freshly isolated cells derived from uninjured or injured muscle. The x-axis shows the number of days after CTX injection. Four to seven independent experiments were performed to calculate the number of each type of cell. (D) Relative expression of *Pax7*, *Myod1* and *Myf5* mRNA was compared between CTX-2d and CTX-5d myogenic cells. The y-axis indicates mean±s.d. (*n*=3 or 4). **P<0.01. (E) Immunostaining of Pax7 (red), MyoD (green) and laminin α2 (LNα2) during skeletal muscle regeneration. Scale bars: 50 μm. White or yellow arrows indicate Pax7$^+$MyoD$^-$ cells located beneath or outside the basal lamina, respectively. The y-axis shows the number of Pax7$^+$MyoD$^-$ (pink), Pax7$^+$MyoD$^+$ (blue) or Pax7$^-$MyoD$^+$ (yellow) cells per mm^2 in TA muscle during regeneration. The x-axis shows the number of days after CTX injection. Cells were counted in two to five fields per mouse; data are average results from three independent mice.
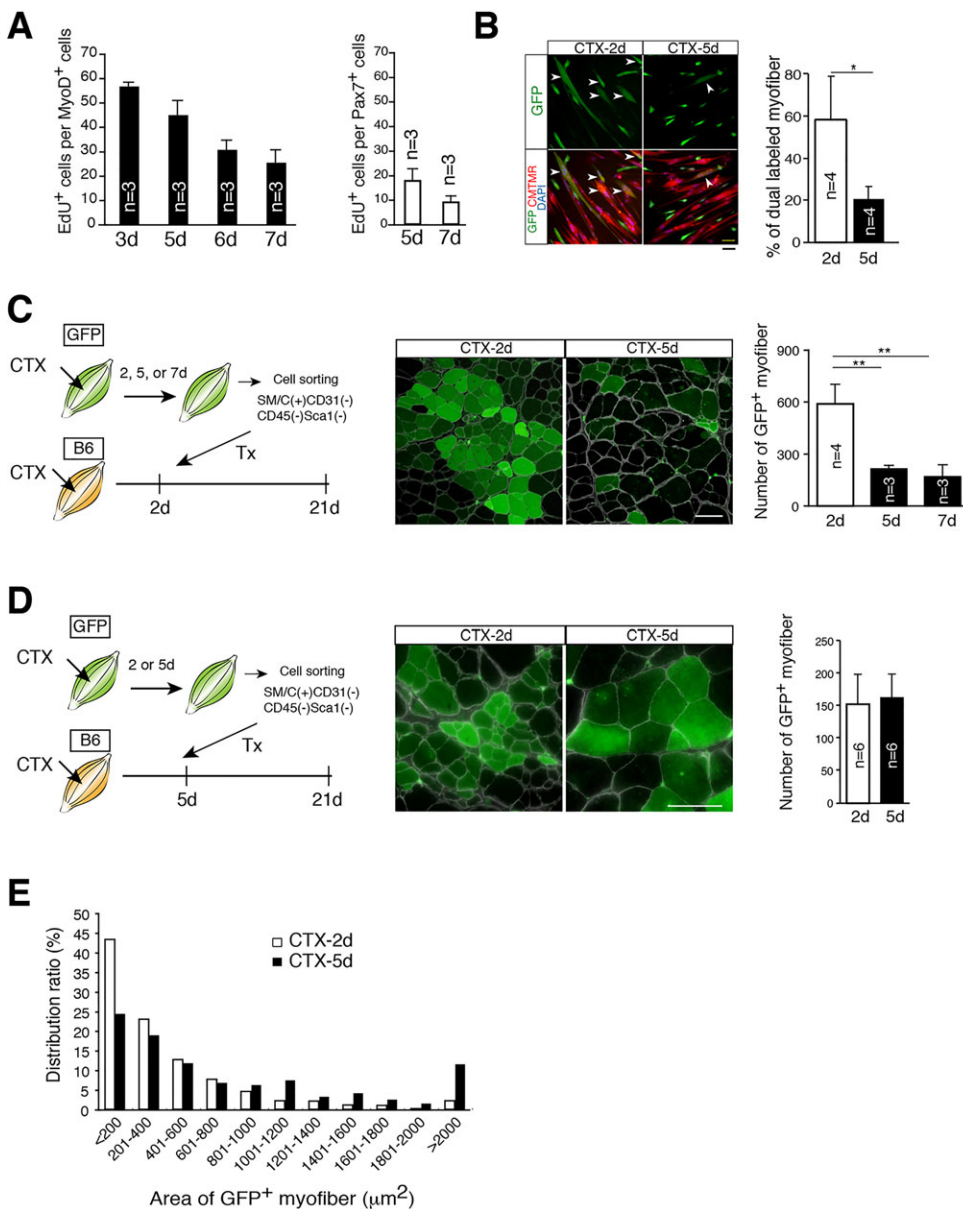
Fig. 2. Functional differences between CTX-2d and CTX-5d myogenic cells. (A) The percentage of EdU$^+$ cells per MyoD$^+$ or Pax7$^+$ cells on the indicated day after CTX injection. EdU was administered 24 h before fixation. (B) Co-culture of CMTMR-labeled myotubes (red) and freshly isolated GFP-tg-derived myogenic cells (green) from regenerating muscle 2 (CTX-2) or 5 (CTX-5) d after CTX injection. Arrowheads indicate the dual-labeled myotubes. Histograms show the percentages of dual-labeled myotubes per CMTMR-labeled myotube. (C,D) The experimental cell transplantation procedure. The muscles of GFP-tg mice were injured by CTX injection; SM/C-2.6$^+$CD31$^-$CD45$^-$Sca-1$^-$ cells (4.5×10^4 cells) were isolated on the indicated day. The cells were injected into TA muscles of C57BL/6 mice 2 (C) or 5 days (D) after CTX injection. The TA muscles were analyzed for expression of GFP (green) and LNα2 (white) 21 days after CTX injection. The histograms show the mean numbers of GFP$^+$ myofibers per section±s.d. (E) The areas of all GFP$^+$ myofibers in D were counted. The histogram shows the distribution of myofibers in the indicated area on the x-axis per total GFP$^+$ myofibers. The number of mice used (A,C,D) or independent experiments (B) is shown in each graph. *$P<0.05$, **$P<0.01$. Scale bars: 50 µm.

cells in MyoD$^+$ cells then gradually decreased as regeneration progressed. When EdU was injected 4 or 6 days after CTX injection, only 17.6% or 8.8% of Pax7$^+$ cells took up EdU during a 24 h pulse-chase. Immunostaining studies of Ki67 in isolated myogenic cells showed similar results (supplementary material Fig. S1C). In addition, the frequencies of EdU$^+$ cells in isolated Pax7$^+$MyoD$^-$ cells and Pax7$^+$MyoD$^+$ cells were 21.8% and 26.3%, respectively; therefore, in spite of MyoD expression levels, Pax7$^+$ cells in CTX-5d muscle did not proliferate more actively than CTX-2d myogenic cells.

Next, the differentiation potential of each type of cell was examined. During 1 week of *in vitro* culture, CTX-5d myogenic cells started to express MyoD and showed a fusion index similar to that of CTX-2d myogenic cells (supplementary material Fig. S2A,B). Therefore, their fusion potential was elucidated by co-culture with myotubes. Myogenic cells from CTX-2d or -5d muscles of GFP-tg mice were purified and co-cultured with myotubes labeled with CMTMR for 40 h; the cells were then fixed, and the fluorescence patterns of GFP and CMTMR were observed. When GFP cells fuse with a CMTMR-labeled myotube, both green

and red fluorescence can be detected in one myotube. As shown in Fig. 2B, double-labeled myotubes were more frequently detected in wells of co-cultured CTX-2d and myotubes compared with those of co-cultured CTX-5d and myotubes. However, as described above, a longer culture allowed CTX-5d myogenic cells to form myotubes normally. Therefore, these results suggest that CTX-5d myogenic cells exhibit delayed fusion with immature myotubes compared with CTX-2d myogenic cells.

Then, we compared the *in vivo* potential for myogenic reconstitution among CTX-2d, CTX-5d and CTX-7d myogenic cells using GFP-tg mice. These cells were transplanted into TA muscles of C57BL/6 mice 2 (Fig. 2C) or 5 days (Fig. 2D) after CTX injection, and the muscles were removed and fixed 21 days after CTX injury. As shown in Fig. 2C, more donor-derived (GFP$^+$) myofibers were detected when CTX-2d myogenic cells were transplanted into CTX-2d muscles compared with CTX-5d or CTX-7d myogenic cells, but similar numbers of GFP$^+$ myofibers were detected when these cells were transplanted into CTX-5d muscles (Fig. 2D). However, large GFP$^+$ myofibers were more frequently detected in muscles transplanted with CTX-5d

myogenic cells than with CTX-2d myogenic cells (Fig. 2E), yet the areas of GFP⁻ myofibers in the two samples were not different (supplementary material Fig. S2C). Collectively, these data clearly indicate that CTX-2d and CTX-5d myogenic cells are different. In addition, these data imply that CTX-5d myogenic cells play a role in the maturation of myofibers for the following reason. Donor-derived cells produce myofibers in two different ways: donor cells may fuse with each other or they may fuse with nascent myofibers. It could be considered that the latter case produces larger GFP⁺ myofibers. Although we cannot rule out other possibilities (proliferation, cell death and others), based on observations of large GFP⁺ myofibers in muscles transplanted with CTX-5d myogenic cells and the timing of the appearance of CTX-5d myogenic cells, one possibility is that CTX-5d myogenic cells more frequently fuse with nascent myofibers rather than with myotubes (such as *in vitro* myotubes).

Doublecortin is specifically expressed in the middle stage of muscle regeneration

In order to identify a marker specific for the middle stage of muscle regeneration, microarray analyses of the myogenic cells derived from CTX-2d and CTX-5d muscle were performed and

compared with our previous data on quiescent satellite cells (Fukada et al., 2007). Finally, we focused on *doublecortin* (*Dcx*), the mutation of which is known to cause human lissencephaly, as the middle stage-specific gene. As shown in Fig. 3A,B, *Dcx* was specifically expressed in the middle stage of muscle regeneration, but not in quiescent satellite cells or in CTX-2d myogenic cells. Two other members of the Dcx family, doublecortin-like kinase 1 (*Dclk1*) and doublecortin-like kinase 2 (*Dclk2*), were also detected in the middle stage of muscle regeneration, but mRNA expression of *Dcx* was the most strictly restricted to the middle stage. The expression of Dcx protein was also detected in myogenic cells of CTX-5d muscles but not in quiescent cells or in cells in early muscle regeneration, and the expression of Dcx protein had disappeared in CTX-28d muscles (Fig. 3C,D; supplementary material Fig. S2D). In addition, 92.8% of Dcx⁺ cells in CTX-5d muscle expressed Pax7, but they rarely expressed either MyoD or myogenin (Fig. 3E). Furthermore, we never observed Dcx⁺ cells in isolated myogenic cells derived from CTX-2d or -3d muscle, and almost no Dcx⁺ CTX-5d myogenic cells expressed MyoD (Fig. 3F). Taken together, these results indicate that Pax7⁺MyoD⁻ myogenic cells in the middle stage of muscle regeneration have different characteristics from
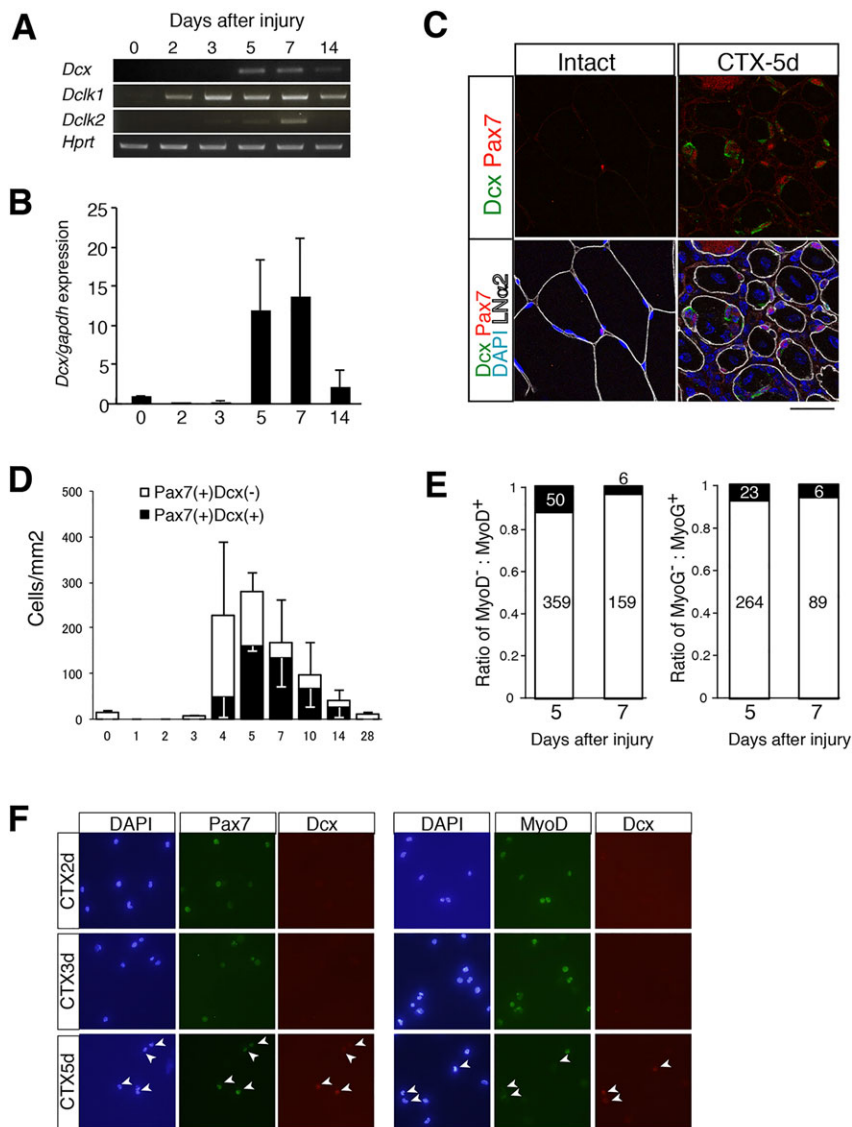

Fig. 3. Doublecortin marked Pax7⁺MyoD⁻ myogenic cells in the middle stage of muscle regeneration. (A) Transcripts of doublecortin (*Dcx*) and doublecortin-related genes (*Dclk1* and *Dclk2*) were quantified by RT-PCR in freshly isolated myogenic cells during skeletal muscle regeneration. *Hprt* was used as a control. (B) Transcripts of the *Dcx* gene were quantified in freshly isolated myogenic cells during skeletal muscle regeneration. Data are mean±s.d. of three independent experiments. (C) Immunostaining of Pax7 (red), Dcx (green), LNα2 (white) and DAPI (blue) in intact TA muscle or CTX-5d TA muscle. Scale bar: 30 μm. (D) Histograms show the numbers of Pax7⁺Dcx⁺ (black column) and Pax7⁺Dcx⁻ (white column) cells per mm² ±s.d. Three mice were used for each sample. (E) Histograms show the frequency of MyoD⁺ or myogenin⁺ (MyoG⁺) cells in Dcx⁺ cells in TA muscle 5 or 7 days after CTX injection. The number in the graph indicates the cells counted. White and black columns show myogenic marker-negative and -positive cells, respectively. Two or three mice were used. (F) Immunostaining of Dcx (red), Pax7 (green) or MyoD (green) in sorted myogenic cells derived from CTX-2d, CTX-3d or CTX-5d muscle. Nuclei are counterstained with DAPI. Arrowheads indicate Pax7⁺Dcx⁺ or MyoD⁻Dcx⁺ cells. Scale bar: 50 μm. The *x*-axis of each graph indicates the number of days after CTX injection (B,D,E).
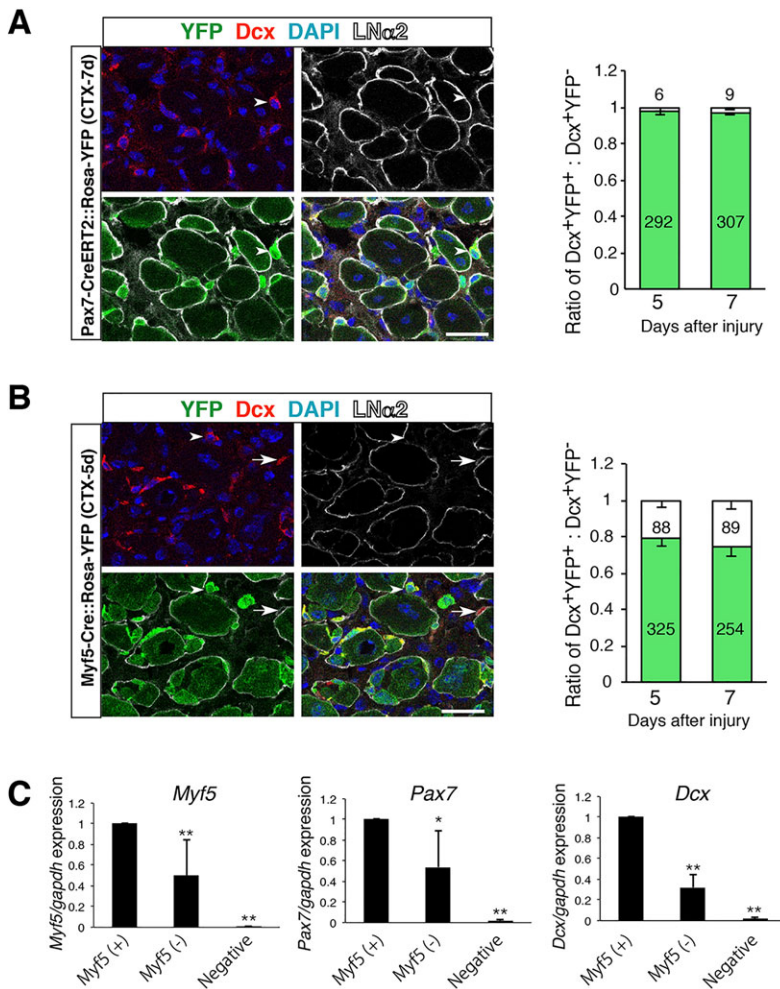
Fig. 4. Doublecortin-positive cells were derived from satellite cells. (A,B) TA muscles of Pax7-CreERT2::Rosa-YFP (A) or Myf5-Cre::Rosa-YFP (B) mice were injured by CTX injection, and the muscles were fixed 5 or 7 days after injury. Pax7-CreERT2::Rosa-YFP mice were treated with tamoxifen 14 days before CTX injection. The sections were stained with anti-YFP (green), Dcx (red), LNα2 (white) and DAPI (blue). Arrowheads indicate Dcx⁺YFP⁺ cells located outside the basal lamina. Arrows indicate Dcx⁺YFP⁻ cells. The histograms show the ratio of YFP⁺ cells to Dcx⁺ cells. The number of cells counted is shown. Two or three mice were used. Scale bars: 25 µm. (C) Transcripts of *Myf5*, *Pax7* or *Dcx* genes were quantified by qRT-PCR in Myf5⁺, Myf5⁻ satellite cells and non-myogenic cells (negative). Three mice were used in this analysis. *$P<0.05$, **$P<0.01$.

quiescent satellite cells and myoblasts, and that they alone express Dcx.

Origin of doublecortin-positive myogenic cells

In order to clarify the origin of Dcx⁺ cells, lineage-tracing experiments were performed. First, Pax7-CreERT2 and Rosa-YFP reporter mice were used to elucidate whether Dcx⁺ cells were derived from quiescent satellite cells or not. Pax7-CreERT2::Rosa-YFP mice were treated with tamoxifen, and 14 days later their muscles were injured by CTX injection. Five or 7 days after CTX injury, Dcx and YFP expressions were examined. As shown in Fig. 4A, almost all Dcx⁺ cells were marked by YFP, which clearly indicates that Dcx⁺ cells originated from quiescent satellite cells, and that Dcx proteins are specifically expressed in myogenic lineage cells in skeletal muscle because Dcx⁺YFP⁻ cells were scarcely detected (Fig. 4A).

Satellite cells can also be divided into two populations by Myf5 expression (Kuang et al., 2007). Kuang et al. demonstrated that Myf5⁻ satellite cells act as 'satellite stem cells' that generate Myf5⁺ satellite cells. Using Myf5-Cre::Rosa-YFP mice, we investigated whether Dcx⁺ myogenic cells are derived from Myf5⁻ cells or not. As shown in Fig. 4B, ~20% of cells detected were Dcx⁺YFP⁻ in CTX-5d and CTX-7d muscle. In addition, Dcx transcripts were also detected in the Myf5⁻ satellite cell fraction, as well as in the Myf5⁺ satellite cell fraction (Fig. 4C). Taken together, these results indicate that both Myf5⁺ and Myf5⁻

satellite cells can generate Dcx⁺ myogenic cells during skeletal muscle regeneration.

Suitable environment-induced expression of doublecortin in myoblasts

Next, in order to examine whether a suitable environment induces Dcx expression in CTX-2d myogenic cells, we transplanted CTX-2d myogenic cells into TA muscles 0.2 or 2 days after CTX injection (Fig. 5A). Before transplantation, Dcx protein was never observed in CTX-2d myogenic cells (Fig. 5B). Three days after cell transplantation, muscles were removed and fixed; therefore, both donor cells were harvested 5 days after activation. As shown in Fig. 5C, ~20% of GFP⁺ mononuclear cells expressed Dcx when donor GFP⁺ cells were transplanted into CTX-2d muscles (Fig. 5B,C). By contrast, when GFP⁺ donor cells were injected into CTX-0.2d muscle, no Dcx⁺GFP⁺ cells were observed (Fig. 5D). Because nearly all transplanted cells (CTX-2d myogenic cells) were Pax7⁺MyoD⁺ cells (Fig. 1D), these results indicate that Pax7⁺MyoD⁺ myoblasts became Dcx⁺ myogenic cells due to specific signals received in the middle stage of regeneration.

Loss of muscle mass after regeneration in doublecortin knockout mice

To examine the role of Dcx during skeletal muscle regeneration, we analyzed *Dcx* knockout (KO) mice. The *Dcx* gene is encoded on the X chromosome, and the male *Dcx* KO mouse is a mild model of human lissencephaly (Corbo et al., 2002). Normally, body and
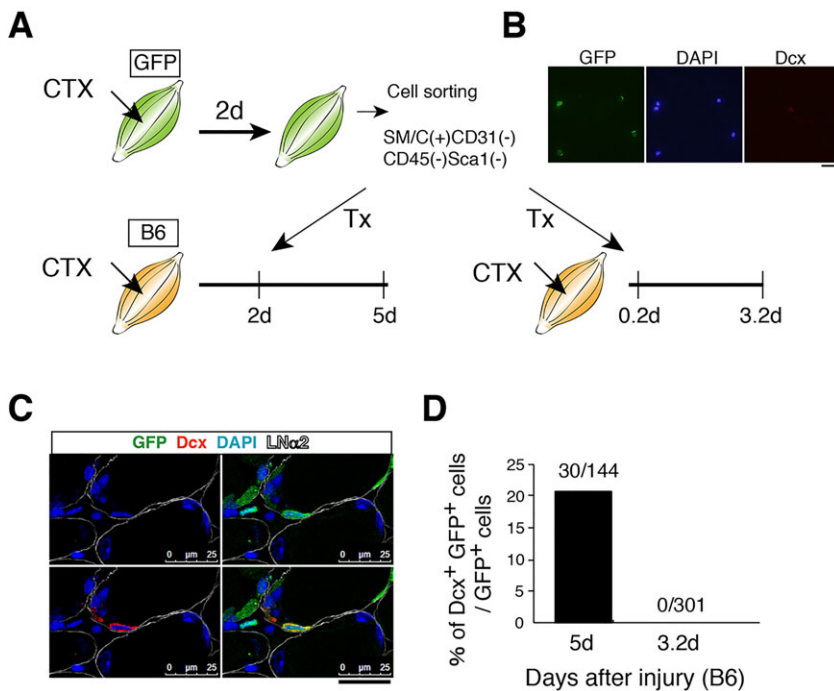
Fig. 5. Microenvironment-induced Dcx expression in Pax7$^+$MyoD$^+$ myoblasts. (A) The experimental cell transplantation procedure. Myogenic cells (4.5×10^4 cells) were prepared from GFP-tg mice after CTX injection. The cells were injected into TA muscles of C57BL/6 mice 2 or 0.2 days after CTX injection. (B) Immunostaining of GFP (green), Dcx (red) and DAPI (blue) in sorted myogenic cells derived from CTX-2d GFP-tg muscle. Scale bar: 50 μm. (C) Five or 3.2 days after CTX injection, the TA muscles were analyzed for expression of GFP (green) Dcx (red), LNα2 (white) and DAPI (blue). Scale bar: 25 μm. (D) The histograms show the percentage of GFP$^+$Dcx$^+$ out of GFP$^+$ cells. The number in the graph indicates the number of cells counted.

muscle weights of *Dcx* KO mice are similar to those of littermate control (wild-type) mice (Fig. 6A,B). Histological studies also demonstrated normal skeletal muscle development in *Dcx* KO mice (Fig. 6C). However, when the muscles were injured, a loss of muscle weight was observed in *Dcx* KO mice 2 weeks after CTX injection (Fig. 6D). By contrast, wild-type mice exhibited a slight increase in muscle weight after CTX injection, as previously observed (Fukada et al., 2011). The number of myofibers in *Dcx* KO mice was not altered (Fig. 6E), but the size of their myofibers was decreased in regenerated muscles compared with those in wild-type mice (Fig. 6C,F). Furthermore, *Dcx* KO mice showed a smaller number of myonuclei than did wild-type mice after regeneration (Fig. 6G). These results indicate that the loss of muscle mass in *Dcx* KO mice resulted from an insufficient supply of myonuclei by mononuclear cells; therefore, Dcx$^+$ myogenic cells likely contribute to maturation of myofibers by providing myonuclei.

Doublecortin and cell location/motility

To elucidate the mechanism that causes the decrease in the accumulation of myonuclei in *Dcx* KO mice, satellite cells were prepared from wild-type and *Dcx* KO mice, and their proliferation and differentiation potentials were examined *in vitro*. However, there was no difference between wild-type and *Dcx* KO cells (supplementary material Fig. S3A,B). *In vivo*, *Dcx* KO mice also had normal myogenic cells and myotubes at 3 and 4 days after CTX injection, respectively (supplementary material Fig. S3C). The results of EdU uptake (supplementary material Fig. S3D) and TUNEL staining (supplementary material Fig. S3E) were also the same in wild-type and *Dcx* KO mice *in vivo* 5 or 7 days after CTX injection. These results indicate that the Dcx defect did not affect myoblast proliferation, myotube formation or survival of myogenic cells.

Satellite cells are defined as mononuclear cells located beneath the basal lamina. However, we found that ~20% of Pax7$^+$ cells are located outside the basal lamina in CTX-5d muscles (Fig. 7A; supplementary material Fig. S4) and that most of them express Dcx (Fig. 7B). Although the frequencies of interstitial Pax7$^+$ cells per total number of Pax7$^+$ cells were similar between CTX-4d and

CTX-5d muscles, the percentage of Dcx$^+$ cells per number of external Pax7$^+$ cells in CTX-4d muscle was much lower than in CTX-5d muscle (Fig. 7B). Therefore, we hypothesized that *Dcx* KO myogenic cells have an impairment in homing in to the proper position. In order to elucidate this hypothesis, the locations of Pax7$^+$ cells in wild-type and *Dcx* KO mice were compared. As shown in Fig. 7C, the frequency of interstitial Pax7$^+$ cells in the CTX-5d muscles did not differ between wild-type and *Dcx* KO mice, but *Dcx* KO mice exhibited increased numbers of interstitial Pax7$^+$ cells 7 days after CTX injection compared with wild-type mice. In addition, the number of Pax7$^+$ cells locating beneath the basal lamina was decreased in *Dcx* KO mice 14 days after CTX injection (Fig. 7D). These results suggest that Dcx expression is related to the homing of interstitial Pax7$^+$ cells.

As shown in Fig. 2, transplantation of CTX-5d myogenic cells into CTX-5d muscles resulted in the generation of large GFP$^+$ myofibers. In order to examine the role of Dcx in this result, control or retrovirally Dcx-expressing myogenic cells were transplanted into *mdx* mice (*Dmd*-mutant mice; a model for Duchenne muscular dystrophy), and the myogenic reconstitution of transplanted cells was examined by counting dystrophin-positive myofibers. As shown in Fig. 7E, the numbers of dystrophin-positive myofibers were similar in control and Dcx-expressing myogenic cells, but the area of dystrophin-positive myofibers in the muscles with transplanted Dcx-expressing cells was larger than that in control cells (Fig. 7F). These results also support the role of Dcx in the maturation of myofibers through homing to a proper location (beneath the basal lamina).

Migration is one of the aspects of cellular homing. As shown in Fig. 7G, Dcx-expressing myogenic cells moved more rapidly than control cells, therefore confirming the promotive effect of Dcx on the motility of myogenic cells. A wound-healing assay also demonstrated the increased cell motility of Dcx-expressing cells (Fig. 7H). In conclusion, these results suggest that Dcx-positive cells are necessary for maturation of myofibers and that Dcx contributes to the homing of myogenic cells into the proper position by accelerating cell migration.
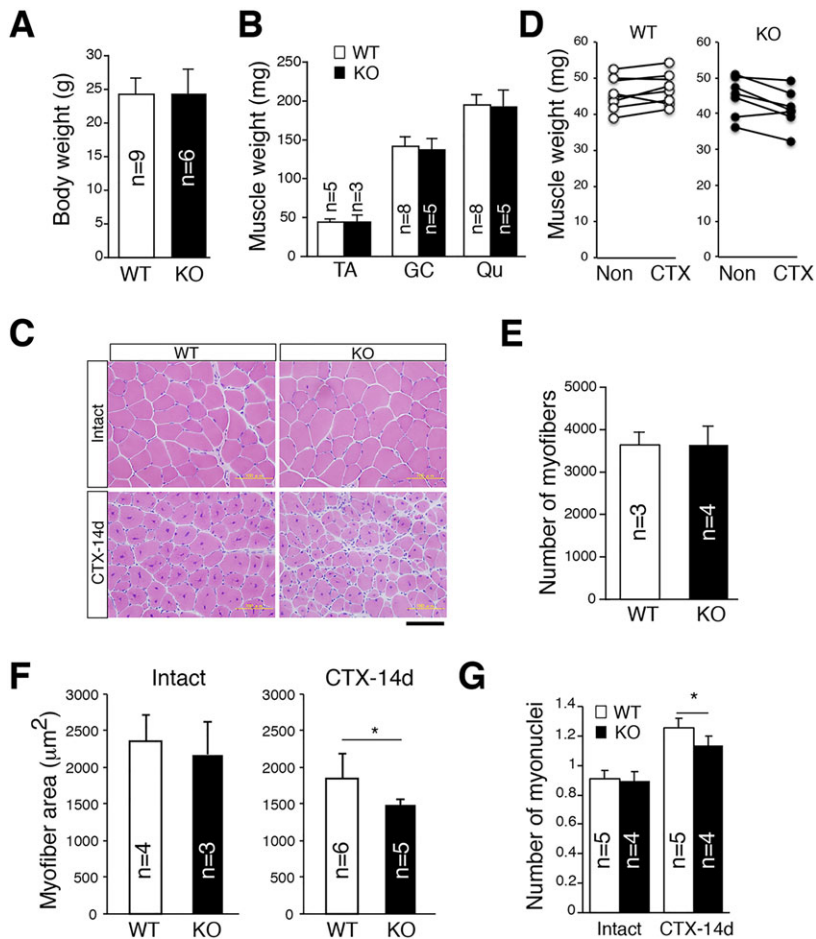
Fig. 6. *Dcx* KO mice exhibited normal growth but impaired muscle regeneration. (A) Body weights of 12-week-old male control littermates (wild-type) and KO mice. Data are mean±s.d. (B) Tibalis anterior (TA), gastrocnemius (GC) and quadriceps femoris (Qu) muscle weights (mg) of 12-week-old male wild-type and KO mice. Data are mean±s.d. (C) Hematoxylin and Eosin staining of intact or injured TA muscle. The right TA muscle of a 10-week-old mouse was injected with CTX, and the muscles were fixed 14 days after injection (CTX-14d). The left muscle was used as intact muscle. Scale bars: 100 μm. (D) The changes in TA muscle weight in 10- to 12-week-old male wild-type (left) and KO mice (right) 14 days after CTX injection. Seven out of nine wild-type mice showed increased (average 2.8%) muscle weight after regeneration. However, six out of seven KO mice showed decreased muscle weight (average 7.5%). (E) The number of myofibers in injured TA muscles of 12-week-old male wild-type and KO mice. Data are mean±s.d. (F) The myofiber area in intact and injured muscles (CTX-14d) of 12-week-old male wild-type and KO mice. Data are mean±s.d. (G) The number of myonuclei per myofiber in uninjured and injured muscles of 12-week-old male wild-type and KO mice. Data are mean±s.d. The number of mice used in each study is shown in each graph. White or black bars indicate wild-type or KO mice, respectively. *$P<0.05$.

DISCUSSION

For tissue regeneration and homeostasis, parenchymal cells are replenished by their own adult stem cells, which accomplish proliferation, differentiation and self-renewal. Skeletal muscle is one representative of tissues with remarkably regenerative ability. In addition, skeletal muscle is an excellent model for cellular differentiation, the study of which was established by *in vitro* culture experiments and observation of skeletal muscle development during embryogenesis. Even *in vitro*, myogenic differentiation is accompanied by drastic changes in cell shape and size as cells fuse with each other. However, *in vitro* culture conditions cannot fully reproduce the regenerative process *in vivo* because fully mature myofibers never appear during *in vitro* culture. As shown here, Pax7$^+$MyoD$^-$ cells are abundant in the middle stage of CTX-induced regeneration, most of them express Dcx and Dcx$^+$ myogenic cells contribute to the maturation of myofibers. By contrast, Dcx$^+$ cells do not appear at any stage of differentiation *in vitro*; therefore, the Pax7$^+$Dcx$^+$ cell is a newly identified *in vivo*-specific myogenic cell and a 'non-classical myoblast' because it has different characteristics (proliferation, differentiation, and Dcx expression) from classical myoblasts.

Dcx is a microtubule-associated protein that is mutated in human X-linked lissencephaly, in which neuronal migration is impaired (des Portes et al., 1998; Gleeson et al., 1998). In neural migration, Dcx functions with dynein (a motor protein) to mediate coupling of the nucleus to the centrosome through microtubules (Tanaka et al., 2004). However, the expression and function of Dcx are limited in other types of cells. This study is the first to demonstrate the function of Dcx in myogenic cells. Pallafacchina

et al. reported that Dcx is expressed in neonatal satellite cells but not in adult satellite cells (Pallafacchina et al., 2010). Consistent with that report, Dcx expression decreased with the growth of mice (supplementary material Fig. S5A). However, the expression of Dcx in neonatal satellite cells is much lower than that in the middle stage of myogenesis (supplementary material Fig. S5A,B). In addition, *Dcx* KO mice exhibit muscles of normal weight and size. These results indicate that Dcx is dispensable for skeletal muscle development. What mechanism induces the expression of Dcx in myogenic cells in the restricted phase? Why is Dcx specifically expressed in the middle stage of muscle regeneration? Our transplantation studies demonstrated that the microenvironment of the middle stage of regeneration converts classical myoblasts to Dcx$^+$ cells. It is proposed that the functions and characteristics of macrophages are altered during the regeneration process. Macrophages have inflammatory features in the early stage and show anti-inflammatory characteristics in the middle stage (Arnold et al., 2007). In addition, extracellular matrix patterns differ in the early and middle stages of regeneration (Bentzinger et al., 2013). Although the Dcx induction mechanism has remained unclear, even in neural cells, analyses of the Dcx promoter have suggested the importance of Wnt signaling for Dcx expression because putative transcription facto-binding sites for lymphoid enhancer factor/T-cell factor (LEF/TCF), which are effectors of the canonical Wnt pathway, are located in the proximal region of the Dcx promoter (Piens et al., 2010). Wnt3a and Wnt7a are major Wnt ligands for muscle regeneration (Brack et al., 2008; Le Grand et al., 2009), but do not induce Dcx protein in cultured myoblasts (data not shown). Elucidating the regulatory
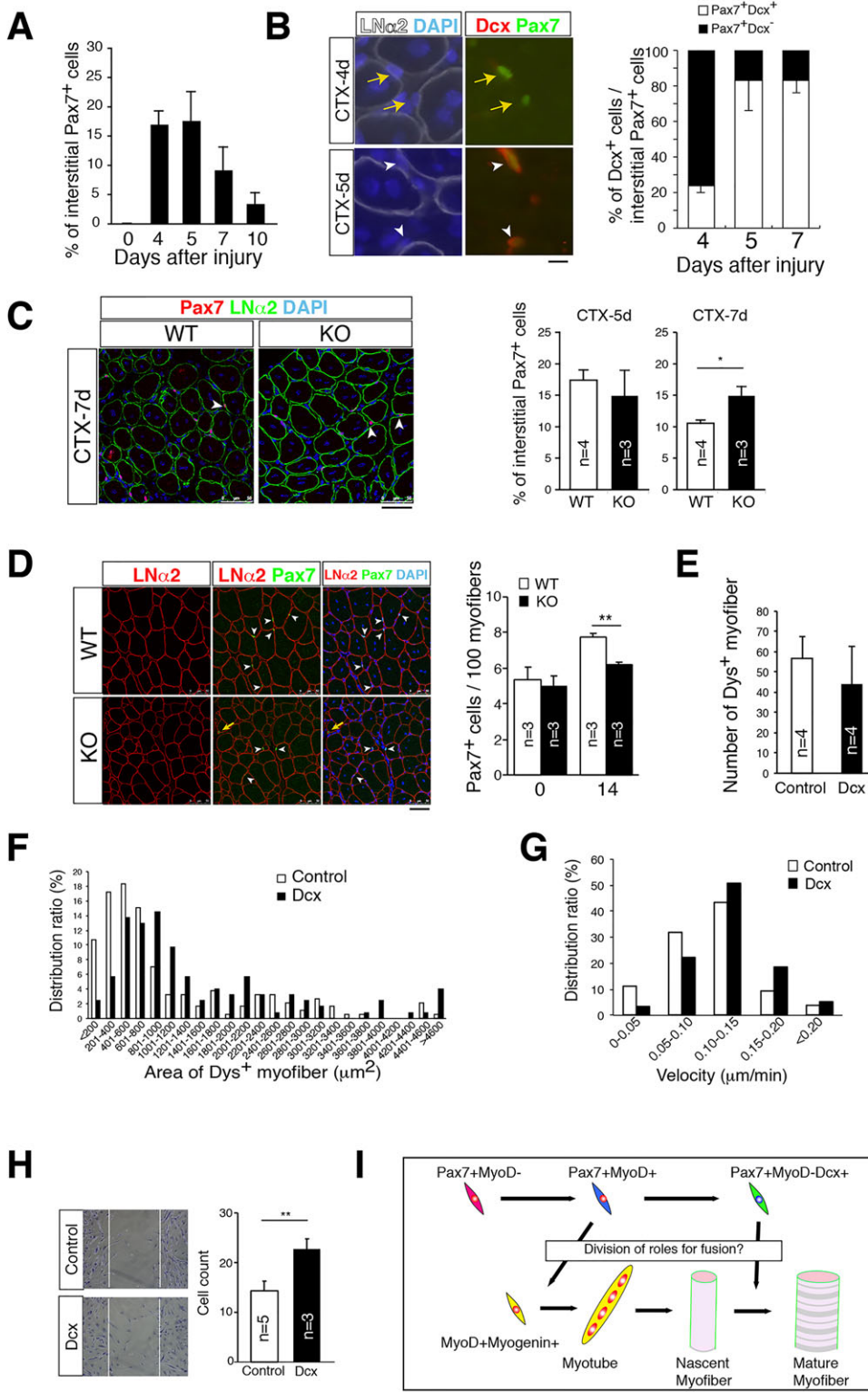
Fig. 7. Dcx promoted migration of myogenic cells. (A) The percentages of Pax7^{+} cells located outside the basal lamina during skeletal muscle regeneration (interstitial Pax7^{+} cells out of total Pax7^{+} cells). Data are mean±s.d. (B) Immunostaining of Pax7 (green), Dcx (red), LNα2 (white) and DAPI (blue) in CTX-4d or CTX-5d muscle. Arrow or arrowhead indicates interstitial Pax7^{+}Dcx[−] or Pax7^{+}Dcx^{+} cells, respectively. Scale bar: 20 µm. Histogram shows the percentages of Dcx^{+} cells out of Pax7^{+} cells located outside the basal lamina. Two or three independent C57BL/6 mice were used. (C) Immunostaining of Pax7 (red), LNα2 (green) and DAPI (blue) in CTX-7d muscle in wild-type or *Dcx* KO mice. Arrowheads indicate interstitial Pax7^{+} cells. Scale bar: 50 µm. Histogram shows the percentage of Pax7^{+} cells located outside the basal lamina out of the total number of Pax7^{+} cells 5 or 7 days after CTX injection. (D) Immunostaining of Pax7 (green), LNα2 (red) and DAPI (blue) in CTX-14d muscle in wild-type or *Dcx* KO mice. Arrowheads indicate Pax7^{+} cells located beneath the basal lamina. Arrows indicate Pax7^{+} cells surrounded by LNα2. Scale bar: 50 µm. Histogram shows the mean number of Pax7^{+} cells per 100 myofibers in uninjured or injured TA muscle of wild type and KO. (E) Control or Dcx-expressing myoblasts were injected into TA muscles of *mdx* (*Dmd*-mutant)mice. Two weeks after the injection, the TA muscles were analyzed for expression of dystrophin (Dys). Data are mean numbers of Dys[+] myofibers per section±s.d. (F) The areas of Dys[+] myofibers in E were counted. Histogram shows the distribution of myofibers in the indicated area on the *x*-axis per total Dys[+] myofibers. (G) Velocity of Dcx-expressing C2C12 or control C2C12 cells. (H) The results of a wound-healing assay. Data are mean number of migrated myoblasts±s.d. (I) The new myogenic differentiation model based on this study. The number of mice used (C-E) or independent experiments (H) are shown in each graph. *$P<0.05$, **$P<0.01$.

mechanisms of Dcx might deepen the understanding of skeletal muscle regenerative processes.

The results of *Dcx* KO mice and expression patterns of Dcx in Pax7 cells in this study suggest that Pax7^{+}Dcx^{+} cells contribute to maturation of myofibers. However, Pax7^{+}Dcx^{+} cells rarely express MyoD or myogenin. Because MyoD and myogenin are considered essential for myogenic cell fusion, their non-expression is puzzling. Myogenin is indispensable for making myofibers;

therefore, in the case of myogenin, there is a possibility that the period in which myogenin protein is detectable was very limited. In contrast to myogenin, studies using *Myod1* KO mice have revealed the existence of a MyoD-independent fusion mechanism that exhibits impaired regeneration with delayed differentiation and that MyoD^{−} myogenic cells differentiate slowly (Megeney et al., 1996; Sabourin et al., 1999). In contrast to *Myod1* KO myoblasts, *Myf5*-KO mice show a mild phenotype and *Myf5*

KO myoblasts tend towards early differentiation (Gayraud-Morel et al., 2007; Montarras et al., 2000). Although MyoD and Myf5 can compensate for each other during skeletal muscle development, their roles appear to be different during skeletal muscle regeneration. Based on these studies, Rudnicki et al. proposed that $MyoD^+$ ($Myf5^-$) myogenic cells contribute to early differentiation (Rudnicki et al., 2008). On the other hand, $MyoD^-$ ($Myf5^+$) myogenic cells differentiate slowly. As shown here, CTX-2d myogenic cells show high MyoD and low Myf5 transcripts compared with CTX-5d myogenic cells. Therefore, classical $Pax7^+MyoD^+$cells and $Pax7^+MyoD^-Dcx^+$ cells are likely to fulfill the characteristics of $MyoD^+Myf5^-$ and $MyoD^-Myf5^+$, respectively.

Thus far, two cell fusion processes have been reported. One is the fusion of mononuclear cell to mononuclear cell, which is the first event in the formation of multinuclear myotubes. The other is the fusion between mononuclear cell and nascent myotube. Horsley et al. indicated that myotubes secrete interleukin 4 (Il4) and recruit Il4 receptor-expressing myoblasts to accelerate myonuclei accumulation (Horsley et al., 2003). They also demonstrated that *Il4* or *Il4ra* KO mice show a decrease in muscle size and myonuclear number, even in uninjured muscles. Inhibition of the Il4rα signal blocks fusion frequency *in vitro*. By contrast, *Dcx* KO mice did not show any impairment in skeletal muscle development. In addition, Dcx induction or depletion did not affect the *in vitro* fusion index, which includes both cell-cell and cell-myotube fusion. Therefore, our results suggest that the fusion of mononuclear cells and nascent myofibers might require mechanisms (Fig. 7I).

In contrast to quiescent satellite cells, ~20% of $Pax7^+$ cells were located outside the basal lamina 5 days after CTX injection, and most of them expressed Dcx. To our knowledge, why and how $Pax7^+$ cells are located outside basal lamina are largely unknown. Recently, Bröhl et al. demonstrated that interstitial $Pax7^+$ cells migrate into the basal lamina during embryonic development and that this process is dependent on Notch signaling (Bröhl et al., 2012). In addition, much evidence indicated that satellite cells can move from outside to inside the basal lamina and vice versa (Collins et al., 2005; Jockusch and Voigt, 2003). Our lineage-tracing experiments also showed that interstitial Dcx^+ cells are derived from satellite cells originally located beneath the basal lamina. Therefore, satellite cells undoubtedly have the potential to traverse the basal lamina and locate in interstitial places. We have not paid attention to the 'interstitial satellite cells' because satellite cells are defined as mononuclear cells located between the basal lamina and myofiber. Therefore, revealing the reason why and mechanisms of how a satellite cell leaves the niche might be fundamental to explaining muscle regeneration.

In conclusion, we identified a $Pax7^+MyoD^-Dcx^+$ myogenic cell possessing different characteristics from classical myoblasts ($Pax7^+MyoD^+$), more committed myogenic cells ($Pax7^-MyoD^+$) and quiescent satellite cells ($Pax7^+MyoD^-$) (supplementary material Fig. S6). Although a fundamental myogenic regeneration process has been established, this non-classical myoblast seems to be essential to fulfill the satellite cell potential. In addition, we examined the function of Dcx in myogenic cells. As in neural progenitors, Dcx promotes cell motility in myogenic cells. Of course, although we cannot rule out the possibility that Dcx has other functions, the mechanism by which Dcx is induced is of interest to fully understand the regeneration of skeletal muscle. This proposed new model might shed light on new methods to improve skeletal muscle regeneration.

MATERIALS AND METHODS
Mice
C57BL/6 mice were purchased from Charles River Japan (Yokohama, Kanagawa, Japan). Heterozygous GFP-tg mice (Okabe et al., 1997) with a C57BL/6 background were maintained in our animal facility by mating with normal C57BL/6 mice. *Dcx* KO mice were generated as previously described (Corbo et al., 2002). Myf5-Cre (Tallquist et al., 2000), Pax7-CreERT2 (Lepper et al., 2009) and Rosa-YFP (Srinivas et al., 2001) mice were obtained from Jackson Laboratories. *mdx* mice (of C57BL/10 background) were provided by Central Laboratories of Experimental Animals (Kanagawa, Japan) and maintained in our animal facility by brother-sister matings. All procedures for experimental animals were approved by the Experimental Animal Care and Use Committee of Osaka University.

Muscle injury
Muscle was injured by injecting 2.5 µl of cardiotoxin in 10 µM saline per gram of mouse body weight (Wako Pure Chemical Industries) into the tibialis anterior muscle. When mononuclear cells were prepared from injured muscles, the cardiotoxin was injected into tibialis anterior (50 µl), gastrocnemius (150 µl) and quadriceps femoris (100 µl) muscles.

Preparation and FACS analyses of skeletal muscle-derived mononuclear cells
Mononuclear cells from skeletal muscles were prepared using 0.2% collagenase type II (Worthington Biochemical) as previously described (Uezumi et al., 2006; Fukada et al., 2004). When myogenic cells from regenerating muscle were prepared, Lympholyte (Cedarlane Laboratories) was used to remove debris following the directions supplied. Detailed information is given in supplementary material Table S1.

Muscle fixation and histological analysis
Tibialis anterior muscles were isolated and frozen in liquid nitrogen-cooled isopentane (Wako Pure Chemical Industries). In order to avoid leaking GFP and YFP proteins, these muscles were fixed in 4% paraformaldehyde for 30 min, immersed sequentially in 10% and 20% sucrose/PBS, and then frozen in isopentane cooled with liquid nitrogen. Transverse cryosections (10 µm) were stained with Hematoxylin and Eosin.

For immunohistological analyses, transverse cryosections (6 µm) were fixed with 4% PFA for 10 min. For eMyHC staining, the sections were fixed with cooled acetone for 10 min at −20°C. Detailed information on antibodies used in this study is listed in supplementary material Table S2. For mouse anti-Pax7 and eMyHC staining, a MOM kit (Vector Laboratories) was used to block endogenous mouse IgG before reacting with the primary antibodies. The signals were recorded photographically using the confocal laser scanning microscope system TCS-SP5 (Leica) or a fluorescence microscope BX51 (Olympus) equipped with a DP70 CCD camera (Olympus).

Immunocytochemistry
FACS-sorted cells collected on glass slides by Cytospin (Thermo Fisher Scientific) or cultured cells were fixed with 4% paraformaldehyde. After permeabilization by 0.25% Triton-X100, the cells were stained with primary antibodies at 4°C overnight and then reacted with secondary antibodies conjugated with Alexa 488 or Alexa 568 (Molecular Probes). Nuclei were stained with 4,6-diamidino-2-phenylindole (DAPI).

RT-PCR
Total RNA was extracted from sorted cells with a Qiagen RNeasy Mini Kit according to the manufacturer's instructions (Qiagen) and then reverse-transcribed into cDNA by using TaqMan Reverse Transcription Reagents (Roche Diagnostics). Real-time PCR was performed using SYBR Premix Ex Taq (Takara) at a final volume of 10 µl. Samples were amplified, and the relative gene expression levels were calculated using standard curves generated by serial dilutions of the cDNA. All primers are listed in supplementary material Table S3.

DEVELOPMENT

Microarray

Target synthesis, gene chip hybridization and data acquisition were performed following our previous study (Fukada et al., 2007). Affymetrix MOE430A GeneChip arrays were used for this analysis. The GEO accession number for our data is GSE56903.

Retroviral vector preparation and infection experiments

A full-length doublecortin cDNA variant 1 was amplified by RT-PCR using following primers including an *Eco*RI or *Not*I site: forward primer, 5′-gaattcacagatgtcaaccgggaa-3′ and reverse primer, 5′-gcggccgcctttcacat-ggaatcgccaa-3′. The PCR product was sequenced and cloned into a bicistronic retrovirus construct, pMXs-IRES/GFP (a kind gift from T. Kitamura, University of Tokyo, Japan) (Kitamura et al., 2003; Nosaka et al., 1999). The viral particles (retro MXs-Dcx-IG and parental retro MXs-IG) were prepared as described previously (Morita et al., 2000). After overnight infection with recombinant retroviruses, the cells were passaged and GFP$^+$ cells were sorted by a FACS Aria II.

Satellite cell culture

Freshly isolated satellite cells were cultured in a growth medium (GM) of high-glucose Dulbecco's modified Eagle's medium (DMEM-HG; Sigma-Aldrich) containing 20% FCS (Trace Biosciences), 10 ng/ml bFGF (PeproTech) and penicillin (100 U/ml)-streptomycin (100 μg/ml) (Gibco BRL) on culture dishes coated with Matrigel (BD Biosciences). Differentiation was induced in differentiation medium (DM) containing DMEM-HG, 5% horse serum and penicillin-streptomycin for 3-4 days.

Cell proliferation assay

To detect the number of proliferating cells *in vivo*, EdU (Invitrogen) was dissolved in PBS at 0.5 mg/ml and injected intraperitoneally at 0.1 mg per 20 g body weight at the time points indicated. The muscles were fixed 24 h after the injection.

To detect the number of proliferating cells *in vitro*, isolated satellite cells were cultured on eight-well Lab-Tek Chamber Slides (Nunc) in GM for 2-3 days and then EdU was added. After additional culture, cells were fixed. EdU was detected following the protocol supplied by the manufacturer.

In vitro fusion index with myotubes

Freshly isolated satellite cells were plated at $1×10^4$ cells per well of eight-well Lab-Tek Chamber slides and grown in GM for 3-4 days. The cells were then cultured in DM to produce myotubes. After 3 days in DM, myotubes were stained with 5 μM CellTracker Orange CMTMR Dye (Molecular Probes) for 20 min at 37°C. Myotubes were washed twice with PBS and cultured for 2-4 h. Myogenic cells derived from CTX-2d or CTX-5d muscle of GFP-tg mice were plated on CMTMR-labeled myotubes. After 40 h, co-cultures were fixed with 4% paraformaldehyde and stained with anti-GFP antibodies.

Detection of apoptosis

Apoptotic cells were detected by rhodamine fluorescence using an ApopTag Red In Situ Apoptosis Detection Kit (Chemicon).

Cell motility assay

The velocity of cell movement was recorded by imaging software (Keyence) and analyzed by ImageJ software. For wound healing assays, $2×10^5$ C2C12 cells were plated on 60 mm fibronectin-coated dishes and cultured. After 1 day in culture, the medium was changed to 0.1% FCS DMEM, and the cells were cultured for 2 additional days. Cells were then scratched with blue chip and the migrated cells were counted after 24 h.

Measurement of myofiber size and myonuclei

ImageJ software was used to measure myofiber size. To calculate the TA myofiber area, 128 to 253 intact or 160 to 255 injured myofibers per mouse were examined. Myonuclei locating inside the basal lamina were counted. By co-staining with anti-M-cadherin, the nuclei of satellite cells or myogenic cells were excluded.

Statistics

Values are expressed as mean±s.d. Statistical significance was assessed using Student's *t*-test. In comparisons of more than two groups, non-repeated measures analysis of variance (ANOVA) followed by the Bonferroni test (versus control) or SNK test (multiple comparisons) were used. A probability of less than 5% ($P<0.05$) or 1% ($P<0.01$) was considered statistically significant.

Supplementary material

Supplementary material available online at
http://dev.biologists.org/lookup/suppl/doi:10.1242/dev.112557/-/DC1

References

Arnold, L., Henry, A., Poron, F., Baba-Amer, Y., van Rooijen, N., Plonquet, A., Gherardi, R. K. and Chazaud, B. (2007). Inflammatory monocytes recruited after skeletal muscle injury switch into antiinflammatory macrophages to support myogenesis. *J. Exp. Med.* **204**, 1057-1069.

Bentzinger, C. F., Wang, Y. X., von Maltzahn, J., Soleimani, V. D., Yin, H. and Rudnicki, M. A. (2013). Fibronectin regulates Wnt7a signaling and satellite cell expansion. *Cell Stem Cell* **12**, 75-87.

Brack, A. S., Conboy, I. M., Conboy, M. J., Shen, J. and Rando, T. A. (2008). A temporal switch from notch to Wnt signaling in muscle stem cells is necessary for normal adult myogenesis. *Cell Stem Cell* **2**, 50-59.

Bröhl, D., Vasyutina, E., Czajkowski, M. T., Griger, J., Rassek, C., Rahn, H.-P., Purfürst, B., Wende, H. and Birchmeier, C. (2012). Colonization of the satellite cell niche by skeletal muscle progenitor cells depends on Notch signals. *Dev. Cell* **23**, 469-481.

Buckingham, M. (2007). Skeletal muscle progenitor cells and the role of Pax genes. *C. R. Biol.* **330**, 530-533.

Cheung, T. H., Quach, N. L., Charville, G. W., Liu, L., Park, L., Edalati, A., Yoo, B., Hoang, P. and Rando, T. A. (2012). Maintenance of muscle stem-cell quiescence by microRNA-489. *Nature* **482**, 524-528.

Collins, C. A., Olsen, I., Zammit, P. S., Heslop, L., Petrie, A., Partridge, T. A. and Morgan, J. E. (2005). Stem cell function, self-renewal, and behavioral heterogeneity of cells from the adult muscle satellite cell niche. *Cell* **122**, 289-301.

Corbo, J. C., Deuel, T. A., Long, J. M., LaPorte, P., Tsai, E., Wynshaw-Boris, A. and Walsh, C. A. (2002). Doublecortin is required in mice for lamination of the hippocampus but not the neocortex. *J. Neurosci.* **22**, 7548-7557.

des Portes, V., Pinard, J. M., Billuart, P., Vinet, M. C., Koulakoff, A., Carrié, A., Gelot, A., Dupuis, E., Motte, J., Berwald-Netter, Y. et al. (1998). A novel CNS gene required for neuronal migration and involved in X-linked subcortical laminar heterotopia and lissencephaly syndrome. *Cell* **92**, 51-61.

Fukada, S., Higuchi, S., Segawa, M., Koda, K.-i., Yamamoto, Y., Tsujikawa, K., Kohama, Y., Uezumi, A., Imamura, M., Miyagoe-Suzuki, Y. et al. (2004). Purification and cell-surface marker characterization of quiescent satellite cells from murine skeletal muscle by a novel monoclonal antibody. *Exp. Cell Res.* **296**, 245-255.

Fukada, S., Uezumi, A., Ikemoto, M., Masuda, S., Segawa, M., Tanimura, N., Yamamoto, H., Miyagoe-Suzuki, Y. and Takeda, S. (2007). Molecular signature of quiescent satellite cells in adult skeletal muscle. *Stem Cells* **25**, 2448-2459.

Fukada, S., Yamaguchi, M., Kokubo, H., Ogawa, R., Uezumi, A., Yoneda, T., Matev, M. M., Motohashi, N., Ito, T., Zolkiewska, A. et al. (2011). Hesr1 and Hesr3 are essential to generate undifferentiated quiescent satellite cells and to maintain satellite cell numbers. *Development* **138**, 4609-4619.

Gayraud-Morel, B., Chrétien, F., Flamant, P., Gomès, D., Zammit, P. S. and Tajbakhsh, S. (2007). A role for the myogenic determination gene Myf5 in adult regenerative myogenesis. *Dev. Biol.* **312**, 13-28.

Gleeson, J. G., Allen, K. M., Fox, J. W., Lamperti, E. D., Berkovic, S., Scheffer, I., Cooper, E. C., Dobyns, W. B., Minnerath, S. R., Ross, M. E. et al. (1998). Doublecortin, a brain-specific gene mutated in human X-linked lissencephaly and double cortex syndrome, encodes a putative signaling protein. *Cell* **92**, 63-72.

Horsley, V., Jansen, K. M., Mills, S. T. and Pavlath, G. K. (2003). IL-4 acts as a myoblast recruitment factor during mammalian muscle growth. *Cell* **113**, 483-494.

Jockusch, H. and Voigt, S. (2003). Migration of adult myogenic precursor cells as revealed by GFP/nLacZ labelling of mouse transplantation chimeras. *J. Cell Sci.* **116**, 1611-1616.

Kitamura, T., Koshino, Y., Shibata, F., Oki, T., Nakajima, H., Nosaka, T. and Kumagai, H. (2003). Retrovirus-mediated gene transfer and expression cloning: powerful tools in functional genomics. *Exp. Hematol.* **31**, 1007-1014.

Kuang, S., Kuroda, K., Le Grand, F. and Rudnicki, M. A. (2007). Asymmetric self-renewal and commitment of satellite stem cells in muscle. *Cell* **129**, 999-1010.

Le Grand, F., Jones, A. E., Seale, V., Scimè, A. and Rudnicki, M. A. (2009). Wnt7a activates the planar cell polarity pathway to drive the symmetric expansion of satellite stem cells. *Cell Stem Cell* **4**, 535-547.

Lepper, C., Conway, S. J. and Fan, C.-M. (2009). Adult satellite cells and embryonic muscle progenitors have distinct genetic requirements. *Nature* **460**, 627-631.

Megeney, L. A., Kablar, B., Garrett, K., Anderson, J. E. and Rudnicki, M. A. (1996). MyoD is required for myogenic stem cell function in adult skeletal muscle. *Genes Dev.* **10**, 1173-1183.

Montarras, D., Lindon, C., Pinset, C. and Domeyne, P. (2000). Cultured myf5 null and myoD null muscle precursor cells display distinct growth defects. *Biol. Cell* **92**, 565-572.

Morita, S., Kojima, T. and Kitamura, T. (2000). Plat-E: an efficient and stable system for transient packaging of retroviruses. *Gene Therapy* **7**, 1063-1066.

Nosaka, T., Kawashima, T., Misawa, K., Ikuta, K., Mui, A. L.-F. and Kitamura, T. (1999). STAT5 as a molecular regulator of proliferation, differentiation and apoptosis in hematopoietic cells. *EMBO J.* **18**, 4754-4765.

Okabe, M., Ikawa, M., Kominami, K., Nakanishi, T. and Nishimune, Y. (1997). 'Green mice' as a source of ubiquitous green cells. *FEBS Lett.* **407**, 313-319.

Pallafacchina, G., François, S., Regnault, B., Czarny, B., Dive, V., Cumano, A., Montarras, D. and Buckingham, M. (2010). An adult tissue-specific stem cell in its niche: a gene profiling analysis of in vivo quiescent and activated muscle satellite cells. *Stem Cell Res.* **4**, 77-91.

Piens, M., Muller, M., Bodson, M., Baudouin, G. and Plumier, J.-C. (2010). A short upstream promoter region mediates transcriptional regulation of the mouse doublecortin gene in differentiating neurons. *BMC Neurosci.* **11**, 64.

Relaix, F., Montarras, D., Zaffran, S., Gayraud-Morel, B., Rocancourt, D., Tajbakhsh, S., Mansouri, A., Cumano, A. and Buckingham, M. (2006). Pax3 and Pax7 have distinct and overlapping functions in adult muscle progenitor cells. *J. Cell Biol.* **172**, 91-102.

Rudnicki, M. A., Le Grand, F., McKinnell, I. and Kuang, S. (2008). The molecular regulation of muscle stem cell function. *Cold Spring Harb. Symp. Quant. Biol.* **73**, 323-331.

Sabourin, L. A. and Rudnicki, M. A. (2000). The molecular regulation of myogenesis. *Clin. Genet.* **57**, 16-25.

Sabourin, L. A., Girgis-Gabardo, A., Seale, P., Asakura, A. and Rudnicki, M. A. (1999). Reduced differentiation potential of primary MyoD-/- myogenic cells derived from adult skeletal muscle. *J. Cell Biol.* **144**, 631-643.

Segawa, M., Fukada, S., Yamamoto, Y., Yahagi, H., Kanematsu, M., Sato, M., Ito, T., Uezumi, A., Hayashi, S., Miyagoe-Suzuki, Y. et al. (2008). Suppression of macrophage functions impairs skeletal muscle regeneration with severe fibrosis. *Exp. Cell Res.* **314**, 3232-3244.

Srinivas, S., Watanabe, T., Lin, C.-S., William, C. M., Tanabe, Y., Jessell, T. M. and Costantini, F. (2001). Cre reporter strains produced by targeted insertion of EYFP and ECFP into the ROSA26 locus. *BMC Dev. Biol.* **1**, 4.

Tallquist, M. D., Weismann, K. E., Hellstrom, M. and Soriano, P. (2000). Early myotome specification regulates PDGFA expression and axial skeleton development. *Development* **127**, 5059-5070.

Tanaka, T., Serneo, F. F., Higgins, C., Gambello, M. J., Wynshaw-Boris, A. and Gleeson, J. G. (2004). Lis1 and doublecortin function with dynein to mediate coupling of the nucleus to the centrosome in neuronal migration. *J. Cell Biol.* **165**, 709-721.

Uezumi, A., Ojima, K., Fukada, S.-i., Ikemoto, M., Masuda, S., Miyagoe-Suzuki, Y. and Takeda, S. (2006). Functional heterogeneity of side population cells in skeletal muscle. *Biochem. Biophys. Res. Commun.* **341**, 864-873.

Zammit, P. S. (2008). All muscle satellite cells are equal, but are some more equal than others? *J. Cell Sci.* **121**, 2975-2982.

Zammit, P. S., Golding, J. P., Nagata, Y., Hudon, V., Partridge, T. A. and Beauchamp, J. R. (2004). Muscle satellite cells adopt divergent fates: a mechanism for self-renewal? *J. Cell Biol.* **166**, 347-357.